

Banner appropriate to article type will appear here in typeset article

Intermittency in turbulent emulsions

M. Cialesi-Esposito¹, G. Boffetta², L. Brandt^{3,4}, S. Chibbaro⁵ and S. Musacchio²

¹INFN, Sezione di Torino, via Pietro Giuria 1, 10125, Torino, Italy

²Dipartimento di Fisica and INFN, Università degli Studi di Torino, via P. Giuria 1, 10125 Torino, Italy.

³FLOW Centre, KTH Royal Institute of Technology, Stockholm, Sweden

⁴Department of Energy and Process Engineering, Norwegian University of Science and Technology(NTNU), Trondheim, Norway

⁵Université Paris-Saclay, CNRS, LISN, 91400 Orsay, France

(Received xx; revised xx; accepted xx)

We investigate the statistics of turbulence in emulsions of two-immiscible fluids of same density. We compute for the first time velocity increments between points conditioned to be located in the same phase or in different phases and examine their probability density functions (PDF) and the associated structure functions (SF). This enables us to demonstrate that the the presence of the interface reduces the skewness of the PDF at scales below the Kolmogorov-Hinze scale and therefore the magnitude of the energy flux towards the dissipative scales, which is quantified by the third-order SF. The analysis of the higher order SFs shows that multiphase turbulence is more intermittent than single-phase turbulence. In particular, the local scaling exponents of the SFs display a saturation about the Kolmogorov-Hinze scale and below, which indicates the presence of large velocity gradients across the interface. Interestingly, the statistics approach of classic homogeneous isotropic turbulence when significantly increasing the viscosity of the dispersed phase.

Key words: Emulsions, multiphase turbulence, intermittency, structure functions.

MSC Codes (*Optional*) Please enter your MSC Codes here

1. Introduction

Emulsions, *i.e.* mixtures composed of two immiscible (totally or partially) liquids with similar densities, are extremely common in industrial applications environment such as pharmaceuticals (Nielloud 2000; Spornath & Aserin 2006), food processing (McClements 2015) and oil production (Kokal & Others 2005; Mandal *et al.* 2010; Kilpatrick 2012). Emulsions are also important in geophysical applications: as example, when oil or industrial wastes spill into water streams (from rivers to oceans), the oil droplet distribution becomes fundamental for quantifying the environmental damage (Li & Garrett 1998; French-McCay 2004; Gopalan & Katz 2010).

At very low-volume-fraction, turbulent emulsions are mainly characterized by the breakup of droplets. The droplet size distribution is produced by the turbulent stresses and the feedback of the dispersed phase on the carrier flow is small, and often neglected. The dynamics of droplet breakup, for a dilute emulsion in a homogeneous and isotropic turbulent flow was initially investigated by Kolmogorov (1949) and Hinze (1955), who derived an expression for the maximum size of droplets resisting breakup as a function of the flow characteristics and the fluid properties. This is usually referred to as the Kolmogorov-Hinze (KH) scale. Recent numerical investigations of droplets, bubbles and emulsions confirmed the general validity of the KH theory, both in isotropic and homogeneous turbulence (Perlekar *et al.* 2014; Mukherjee *et al.* 2019; Rivière *et al.* 2021; Crialesi-Esposito *et al.* 2022b; Giroto *et al.* 2022; Begemann *et al.* 2022), and in anisotropic flows (Soligo *et al.* 2019; Rosti *et al.* 2020; Pandey *et al.* 2022), while some theoretical corrections were lately proposed to account for scale-local nature of the process (Crialesi-Esposito *et al.* 2022a; Qi *et al.* 2022).

At finite volume fraction of the dispersed phase, the distribution of the droplet sizes results from the interplay between breakup and coalescence. In this regime, the presence of droplets also modulates the underlying turbulence, affecting the flow statistics both at large (Yi *et al.* 2021; Wang *et al.* 2022) and small scales (Mukherjee *et al.* 2019; Freund & Ferrante 2019; Vela-Martín & Avila 2021; Crialesi-Esposito *et al.* 2022b). In particular, the presence of a dispersed phase alters significantly the statistics at the small scales, producing large deviations from the average values of dissipation and vorticity (Crialesi-Esposito *et al.* 2022b).

In this work, we address the effects of the dispersed phase on the velocity increments of the turbulent flow at moderate (10%) and high (50%) volume fractions. We study the role of the interface separating the two phases by examining the statistics of velocity increments between two points which are conditioned to be either in the same phase or in different phases. We find that the most important deviations from the statistics of single-phase flows, quantified by the PDFs of the velocity increments, are concentrated in regions around the interface, i.e. when the two points belongs to different phases. Moreover, we show that the amplitude of the third-order structure function (SF) is reduced because of the contribution of the points located around the interface. This is associated with a reduction of the flux of kinetic energy in the turbulent cascade, which, in combination with the surface tension term, alters significantly the energy transport across scales. Finally, we discuss the effects of the droplets on the local scaling exponents of the high-order structure functions, which display a striking saturation at small scales.

The remaining of this paper is organized as follows. In Section 2 we introduce the numerical method adopted for the simulations, Section 3 is devoted to the presentation of the results and Section 4 summarises the main conclusions.

2. Methodology

We consider the velocity field $\mathbf{u}(\mathbf{x}, t)$ obeying the Navier-Stokes equations

$$\rho (\partial_t \mathbf{u} + \mathbf{u} \cdot \nabla \mathbf{u}) = -\nabla p + \nabla \cdot \left[\mu \left(\nabla \mathbf{u} + \nabla \mathbf{u}^T \right) \right] + \mathbf{f}^\sigma + \mathbf{f} \quad (2.1)$$

and the incompressibility condition $\nabla \cdot \mathbf{u} = 0$. In Equation (2.1) p is the pressure and ρ is the density and $\mu(\mathbf{x}, t)$ is the local viscosity. The surface tension force is represented by the term $\mathbf{f}^\sigma = \sigma \xi \delta_S \mathbf{n}$ where σ is the surface tension coefficient, ξ is the local interface curvature, \mathbf{n} the surface normal unit vector and δ_S represents a delta function which ensures that the surface force is applied at the interface only (Tryggvason *et al.* 2011). The last term \mathbf{f} is a constant in time body force which sustains turbulence by injecting energy at large scales. Here, we adopt the so-called ABC forcing (Mininni *et al.* 2006) which reads

$\mathbf{f} = (A \sin(k_f z) + C \cos(k_f y), B \sin(k_f x) + A \cos(k_f z), C \sin(k_f y) + B \cos(k_f x))$. The forcing scale is given by $L_f = 2\pi/k_f$.

We solve Equation (2.1) in a triply-periodic, cubic domain of size $L = 2\pi$, discretized on a staggered uniform Cartesian grid. Spatial derivatives are discretized with a second-order centered finite difference scheme and time integration performed by means of a second-order Adam-Bashford scheme. To reconstruct the interface, we use the algebraic Volume of Fluid method, MTHINC, introduced by Li et al. (2012). A constant-coefficient Poisson equation is obtained using the pressure splitting method (Dodd & Ferrante 2014), which is solved using a Fast Fourier Transform direct solver. All the simulations have been performed with the code FluTAS, described in Cialesi-Esposito et al. (2023), where further details on the numerical methods employed in this study can be found.

We consider four different cases, all using a fixed ABC forcing with $A = B = C = 1$ and $k_f = 2\pi/L_f = 2$. The reference single phase (SP) simulation assumes viscosity $\mu = 0.006$, corresponding to a Taylor-scale Reynolds number $Re_\lambda = 15k^2/(\nu\varepsilon)^{1/2} \approx 137$, with $\varepsilon = \nu\langle(\nabla\mathbf{u})^2\rangle$ the energy dissipation rate, k the turbulent kinetic energy and ν the kinematic viscosity. We vary the volume fraction $\alpha = V_d/V$, defined as the ratio between the volume of the dispersed phase V_d and the total volume $V = L^3$, and the viscosity ratio $\gamma = \mu_d/\mu_c$. As regards different volume fractions, we analyze the two cases with $\alpha = 0.1$ (hereafter MP10) and $\alpha = 0.5$ (hereafter MP50), while keeping $\gamma = 1$ for both cases. Finally, we study the case $\alpha = 0.1$ and $\gamma = 100$ (hereafter MPM). For all multiphase (MP) simulations the density ratio among the two phases is kept equal to 1 and the Weber number $We = \rho L_f u_{rms}^2/\sigma = 42.6$.

All the simulations are performed at a resolution $N = 512$ which is sufficient to resolve all the scales (see Cialesi-Esposito et al. 2022b); statistics are accumulated over several large eddy turnover times $T = L_f/u_{rms}$ once statistical stationary conditions have been reached. For further details on the simulation setup, we refer the reader to Cialesi-Esposito et al. (2022b).

3. Statistics of the multiphase flow

In turbulent multiphase flows, part of the kinetic energy of the carrier phase is absorbed at large scales by the deformation and breakup of the interface of the dispersed phase, while the coalescence of small droplets, their surface oscillations and relaxation from high local curvature re-inject energy in the carrier phase at scales smaller than the Kolmogorov-Hinze scale (Cialesi-Esposito et al. 2022a). The consequences of this complex exchange of energy between the two phases are evident in the kinetic energy spectrum shown in Figure 1. Comparing the spectra of a multiphase flow with that of a single-phase flow sustained by the same forcing, we observe a suppression of energy at low wavenumbers (i.e. large scales) and an enhancement at high wavenumbers. This effect increases with the volume fraction α of the dispersed phase (Mukherjee et al. 2019; Cialesi-Esposito et al. 2022b).

Because of the injection of energy at small scales, due to the droplet dynamics, we expect higher intermittency of the velocity fluctuations in the MP flow than in the SP flow at fixed amplitude of the external forcing. In order to quantify this effect we compute the probability density functions (PDF) of the longitudinal velocity increments $\delta_\ell u = (\mathbf{u}(\mathbf{x}_2) - \mathbf{u}(\mathbf{x}_1)) \cdot (\mathbf{x}_2 - \mathbf{x}_1)/\ell$ at distance $\ell = |\mathbf{x}_2 - \mathbf{x}_1|$. The comparison of the PDFs at two scales within the inertial range, shown in Figure 2, confirms that the velocity increments have larger fluctuations in the case of MP flows, in particular at smaller values of ℓ . This effect increases with the concentration α of the dispersed phase. We also observe that in the case $\gamma = 100$ (i.e. when the dispersed phase is much more viscous than the carrier phase) the effect of the droplets on the velocity increments vanishes due to the damping of fluctuations in the dispersed phase, and we recover the statistics of the SP flow.

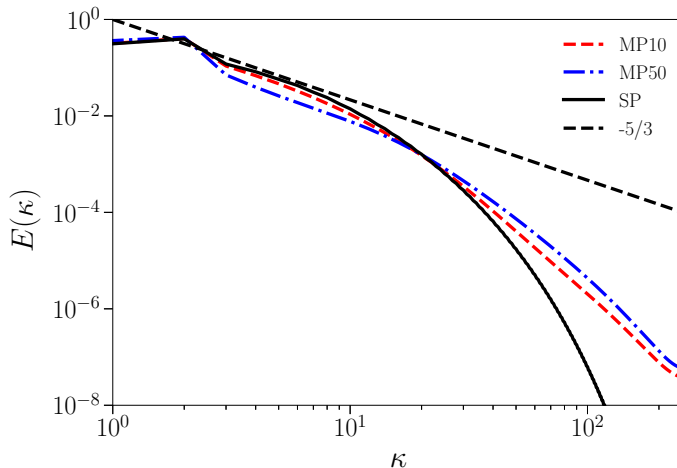


Figure 1: Kinetic energy spectra of SP flow (black continuous line), and MP flows at $\alpha = 0.1$ (red dashed line) and $\alpha = 0.5$ (blue dash-dotted line)

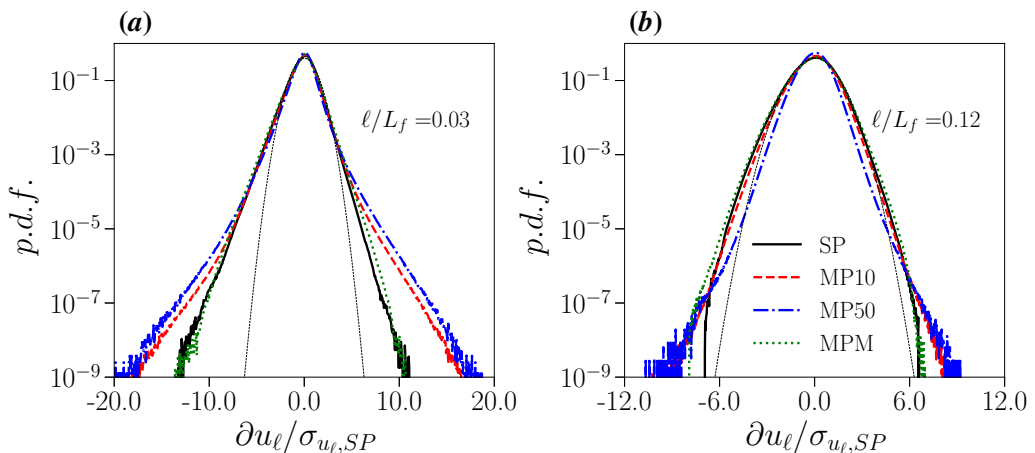


Figure 2: PDF of velocity increments at distance $\ell = 0.03L_f$ (left panel) and $\ell = 0.12L_f$ (right panel), normalized by the standard deviation of the SP case. The single-phase Kolmogorov scale is at $\ell \approx 0.008L_f$

Note that the PDF shown in Figure 2 are computed over the full simulation domain, i.e. the velocity increments are computed among points $\mathbf{x}_{1,2}$ which can belong to both phases unconditionally. To understand the role of the interface in the turbulent statistics, we therefore compute the PDF of the velocity increments conditioned to points belonging to the same or to different phases. Hence, we introduce three different PDFs of the velocity increments depending on which phase the two points \mathbf{x}_1 and \mathbf{x}_2 belong to. We denote by P_{cc} , P_{dd} and P_{cd} the PDFs relative to points belonging only to the carrier phase c , only to the dilute phase d and to both phases, respectively. We remark that, for small values of α , the statistics in the two phases are different. For $\alpha = 0.5$ and $\gamma = 1$ the two phases are equivalent and therefore $P_{dd} = P_{cc}$.

Figure 3 (panels a, b) shows the conditional PDF (normalized with the corresponding variance of the SP case) pertaining the simulation with volume fraction $\alpha = 0.1$. First, we note that the PDF of the carrier phase is not too far from that of the SP case (and this is the case

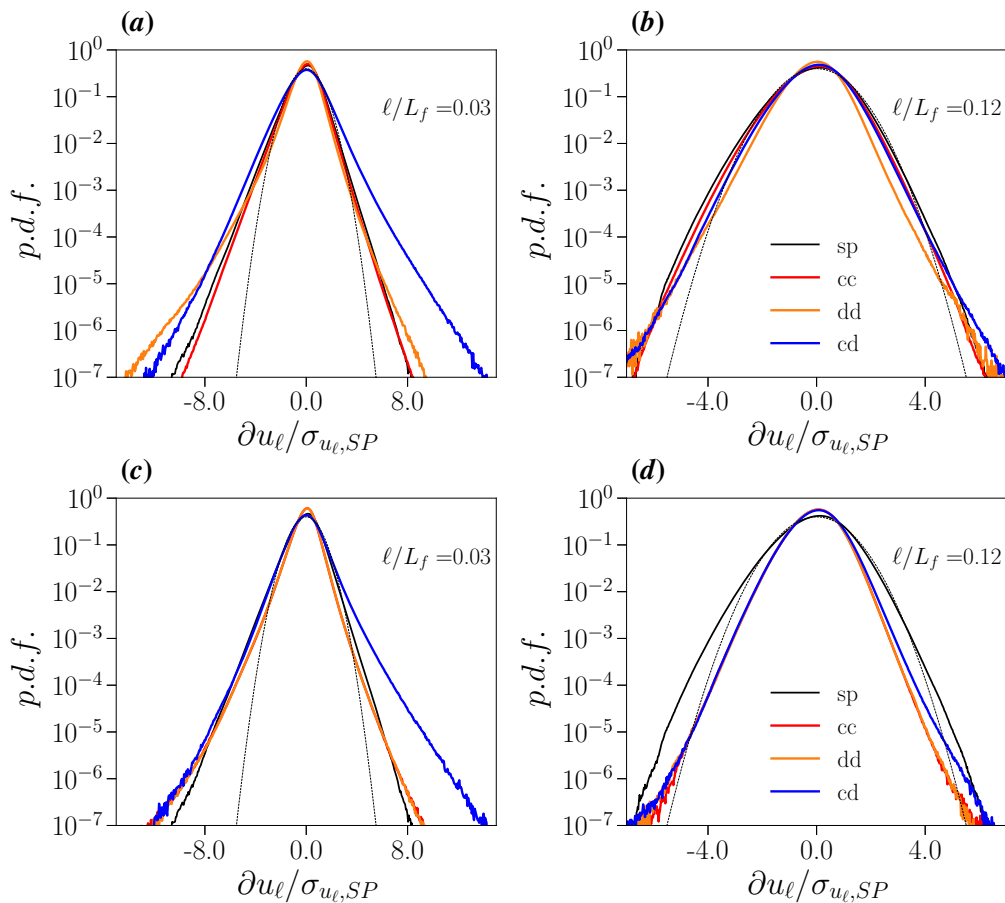


Figure 3: PDFs of velocity increments conditioned to the phases on which the two velocities are measured: cc (both points in the carrier phase, red line), dd (both points in the dispersed phase, orange line), cd (one point in each phase, blue line). Upper panel: Simulation MP10 with $\alpha = 0.1$ and $\gamma = 1$. Lower panel: Simulation MP50 with $\alpha = 0.5$ and $\gamma = 1$. Black line: PDF of velocity increments for a single-phase simulation with the same parameters of the MP simulation. Dashed black line: Gaussian distribution. All the PDFs are rescaled with the variance of the SP case.

also for the variance). In the dispersed phase, on the contrary, velocity increments develop relatively larger tails at small separations. Remarkably, the PDF P_{cd} develops the largest tails at small scale (panel *a*), a clear indication of the role of the interface for small-scale intermittency in MP flows.

Similar observations can be made for the emulsion with $\alpha = 0.5$, shown in Figure 3 (panels *c*, *d*). As expected $P_{cc} = P_{dd}$, and also in this case the data show that the leading contribution to the increased intermittency at small scales comes from velocity increments across the interface, P_{cd} . Note that, although the shapes of P_{cd} are similar for MP10 and MP50, their contribution to the overall flow statistics is different because of the different statistical weight (i.e. the different extension of the total interface).

A remarkable feature shown in Figure 3 is that the skewness of P_{cd} at small scales is opposite (i.e. positive) to that of P_{cc} . We remind that the sign of the skewness is linked to the direction of the turbulent energy cascade via the third-order velocity structure function (SF) defined as $S_3(\ell) = \langle (\delta_\ell u)^3 \rangle$. In the case of SP flows, under the assumption of statistical

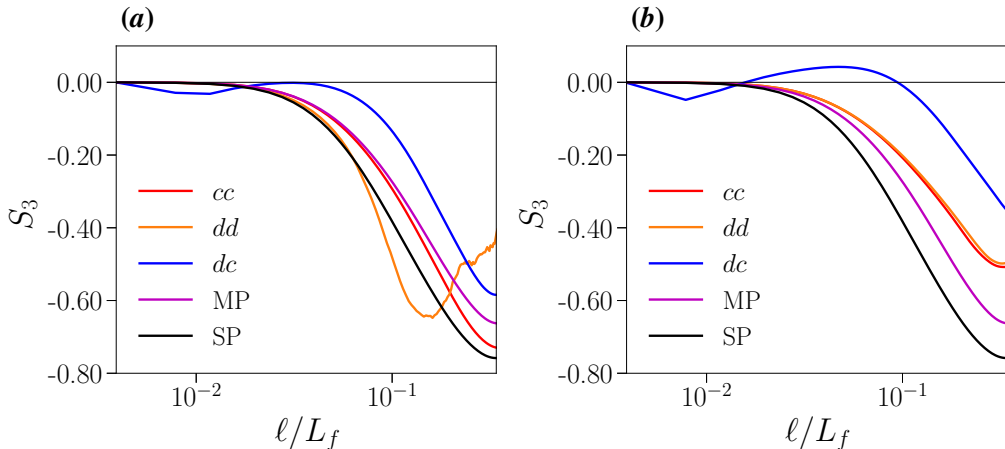


Figure 4: Third-order structure function $S_3(\ell)$ averaged on the whole domain (violet line) or conditioned on the two phases of the flows. Simulation with $\alpha = 0.1$ (left panel) $\alpha = 0.5$ (right panel) and $\gamma = 1$. The black line represents the SP case.

stationarity, homogeneity and isotropy, the Kolmogorov 4/5 law gives $S_3(\ell) = -(4/5)\varepsilon\ell$, where the viscous energy dissipation rate ε is equal to the flux of the turbulent cascade (Frisch 1995). The negative skewness of the PDF of the longitudinal velocity increments is therefore related to the direction of the energy transfer and the negative amplitude of $S_3(\ell)$ is proportional to the energy flux.

In MP flows, because of the opposite sign of the skewness of P_{cd} with respect to P_{cc} , we expect that the presence of the interface reduces the energy flux associated to the turbulent cascade. This can be quantified by looking at the third-order velocity structure function $S_3(\ell) = \langle (\delta_\ell u)^3 \rangle$, whose average can be unconditioned, or conditioned to two points belonging either to the carrier phase $S_3^{cc}(\ell)$, or to the dispersed phase $S_3^{dd}(\ell)$, or points located on different sides of the interface $S_3^{dc}(\ell)$. These are shown in Figure 4.

We see in the figure that the third-order SF of the MP turbulent flows is qualitatively similar to the SP flow when averaged over the whole domain, yet with a smaller amplitude. This is due the fact that part of the turbulence energy is used to break the interface and the direct transfer of energy to small scales is reduced (Craiesi-Esposito et al. 2022b). If we consider the same quantity averaged over one of the two phases only: $S_3^{cc}(\ell)$ and $S_3^{dd}(\ell)$, which are equivalent in a binary flow, the magnitude of the flux increases and approaches the SP limit, indicating that the turbulent cascade is not significantly affected when considering flow structures living in one of the two phases. On the contrary, the flux across two points belonging to different phases is strongly suppressed: the associated $S_3^{dc}(\ell)$ is closer to zero and even changes sign at intermediate scales for $\alpha = 0.5$ (consistently with what suggested in Figure 3). The physical interpretation is that the interface “decouples” the velocity fields in the two phases which become less correlated and therefore with a reduced energy flux, signaled by the reduction of $S_3(\ell)$. The precise behavior of $S_3^{dc}(\ell)$ depends on the value of α , as shown by the comparison with the case $\alpha = 0.1$ (see Figure 4, left panel). Positive values of $S_3^{dc}(\ell)$, hint however to the possibility of scale-local backscatter, which becomes more relevant at increasing volume fractions. Nevertheless, the reduction of the energy flux at intermediate scales is a general feature, independent on α .

The effects of the presence of a dispersed phase on the statistics of the velocity fluctuations affects also the scaling behavior of the structure functions of the absolute values of the longitudinal velocity increments defined as $S_p^a(\ell) = \langle |\delta_\ell u|^p \rangle$. It is well known that in SP

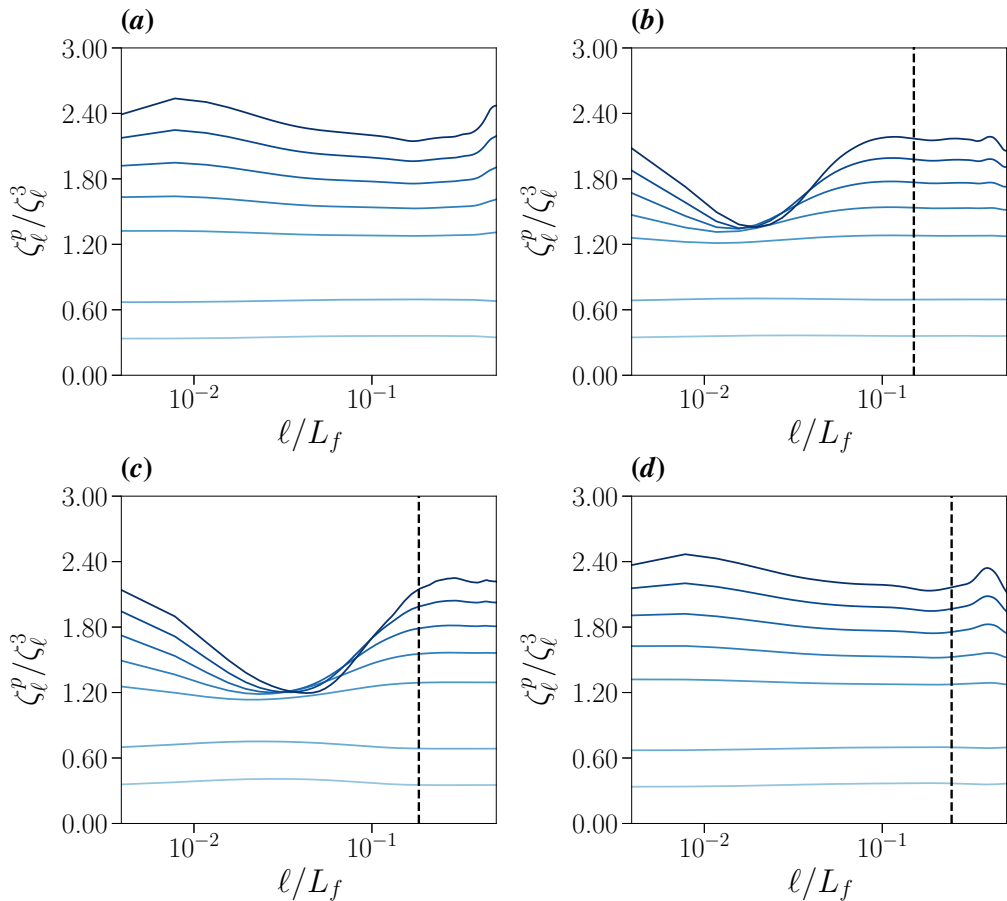


Figure 5: Local scaling exponents ζ_p of the structure functions, for the single phase (Upper left panel), case MP10 at $\alpha = 0.1$ (Upper right panel), case MP50 at $\alpha = 0.5$ (Lower left panel), case MPM at $\gamma = 100$ (Lower right panel). In each figure, the exponents of different order p assume increasing values. Vertical black dashed lines represent the Kolmogorov-Hinze scale, computed in Ciraiesi-Esposito *et al.* (2022a). Curves for $p = 3$ is omitted.

flows the SFs display a power-law behavior $S_p^a(\ell) \sim \ell^{\zeta^p}$ at scales ℓ in the inertial range (Frisch 1995). In this context, intermittency manifests in the non-linear behavior of the scaling exponents: $\zeta^p \neq p/3$. In the MP flows, because of the different physical processes which occur at scales larger and smaller than the Kolmogorov-Hinze scale (dominated by break-up and coalescence respectively), we expect to observe a more complex scaling behavior. To address this issue, we compute the *local scaling exponents* defined as the logarithmic derivative of the SFs $\zeta_\ell^p = d \log(S_p^a(\ell)) / d \log(\ell)$ and here applied to multiphase flows for the first time.

The local scaling exponents ζ_ℓ^p are displayed for $p \leq 8$ in figure 5, where they are divided by the reference scaling exponent ζ_ℓ^3 of the third order SF. In the SP case, panel *a*, we find that the ratios $\zeta_\ell^p / \zeta_\ell^3$ are almost constant in the inertial range $0.09 \leq \ell / L_f \leq 0.32$. In the MP flows, the value of the exponents are a little smaller but comparable to that of the SP case only at large scales; we observe a dramatic decrease of the scaling exponents at scales ℓ smaller than the KH scale $L_{KH} \approx 0.14L_f$ for the case MP10 (panel *b*) and $L_{KH} \approx 0.19L_f$

for the case MP50 (panel *b*) (see vertical line in figure). In particular, we observe a striking saturation of the scaling exponents of the high-order SF with $p \geq 5$ at scales $\ell \approx 0.02L_f$ for the MP50 case and $\ell \approx 0.04L_f$ for the MP10 case. The saturation of the scaling exponents of the high order SFs reveals the presence of strong velocity differences across the interface between the two phases, which originates from the pressure jump at the interface caused by the surface tension forces.

Note also that the saturation of the exponents is not observed when the dispersed phase presents higher viscosity, case MPM in panel *d*. This is consistent with the previous observations in Figure 2, showing that when velocity gradients across the interface are significantly reduced (e.g. by higher viscosity) no exponent saturation is observed.

4. Conclusions

We have discussed intermittency and scaling exponent obtained from direct numerical simulations (DNS) of turbulent emulsions at moderate (10%) and high (50%) volume fractions and two different values of the viscosity contrast. As observed in previous works (Perlekar 2019; Pandey et al. 2020; Cialesi-Esposito et al. 2022b), the presence of a deformable interface increases the intermittency in the flow and the energy content at small scales, when the surface tension offers an alternative path for energy transport across scales.

By investigating the statistics of the velocity increments conditioned to points belonging to a single phase or to different phases, we demonstrate that the increased intermittency is mostly due to the presence of strong velocity differences across the interface between the carrier and the dispersed phase.

We also show that the presence of the dispersed phase causes a decrease of the negative skewness of the PDF of the longitudinal velocity increments. This is associated with a reduction of the flux of the kinetic energy from the forcing scale to the viscous scales. In other words, the presence of a deformable interface affects the vortex stretching and tilting associated to the classic turbulent energy cascade of single-phase flows.

This effect becomes remarkable at the highest volume fraction considered here, when the flux related to points lying on either side of the interface gives a positive contribution to the distribution skewness. This suggests a not-negligible backscatter in multiphase flows, expected in proximity of the interface separating the two fluids. We interpret this reduced flux as due to the absorption and dissipation of part of the kinetic energy of the turbulent flow by the deformation and break-up of drops of the dispersed phase.

Finally, to understand the local properties of turbulence, we have analysed the longitudinal Structure Functions at higher orders. Interestingly, at scales larger than the Kolmogorov-Hinze, the exponents are only slightly smaller than in the single-phase flow, which implies increased intermittency, yet a similar anomalous scaling. More importantly, we report a neat saturation of the exponents for structure functions higher than 3 at scales smaller than the Kolmogorov-Hinze length. This is typically related to a strongly intermittent dynamics and to the presence of jumps, here due to the pressure differences across the interface induced by the surface tension.

A further demonstration that the interface is responsible of the increased intermittency is given by the results for the flow at viscosity ratio $\gamma = 100$. In this case, small-scale fluctuations are damped, especially in the more viscous dispersed phase, and the statistics approach those of the single-phase turbulence with no exponent saturation.

These observations may prove fundamental for understanding small scale dynamics in multiphase flows and for their future sub-grid modelling. Indeed, our results indicate that a correct model would need to account for the reduction of the energy fluxes near an interface. Moreover, we have shown that the turbulence statistics approach those of the single-phase

flow when the droplets consist of a highly viscous fluid. This suggests that, despite several global measures seem to indicate a similar dynamics (Olivieri et al. 2022; Yousefi 2022), the turbulence modulation is significantly different in the case of rigid particles and deformable intrusions.

REFERENCES

- BEGEMANN, ALEXANDER, TRUMMLER, THERESA, TRAUTNER, ELIAS, HASSLBERGER, JOSEF & KLEIN, MARKUS 2022 Effect of turbulence intensity and surface tension on the emulsification process and its stationary state—a numerical study. *The Canadian Journal of Chemical Engineering* **100** (12), 3548–3561.
- CRIALESI-ESPOSITO, MARCO, CHIBBARO, SERGIO & BRANDT, LUCA 2022a The interaction of droplet dynamics and turbulence cascade. *arXiv preprint arXiv:2206.08055*.
- CRIALESI-ESPOSITO, MARCO, ROSTI, MARCO EDOARDO, CHIBBARO, SERGIO & BRANDT, LUCA 2022b Modulation of homogeneous and isotropic turbulence in emulsions. *Journal of Fluid Mechanics* **940**, A19.
- CRIALESI-ESPOSITO, MARCO, SCAPIN, NICOLÒ, DEMOU, ANDREAS D., ROSTI, MARCO EDOARDO, COSTA, PEDRO, SPIGA, FILIPPO & BRANDT, LUCA 2023 Flutas: A gpu-accelerated finite difference code for multiphase flows. *Computer Physics Communications* **284**, 108602.
- DODD, MICHAEL S. & FERRANTE, ANTONINO 2014 A fast pressure-correction method for incompressible two-fluid flows. *Journal of Computational Physics* **273**, 416–434.
- FRENCH-McCAY, DEBORAH P 2004 Oil spill impact modeling: development and validation. *Environmental Toxicology and Chemistry: An International Journal* **23** (10), 2441–2456.
- FREUND, ANDREAS & FERRANTE, ANTONINO 2019 Wavelet-spectral analysis of droplet-laden isotropic turbulence. *J. Fluid Mech* **875**, 914–928.
- FRISCH, URIEL 1995 Turbulence. Cambridge University Press.
- GIROTTO, IVAN, BENZI, ROBERTO, DI STASO, GIANLUCA, SCAGLIARINI, ANDREA, SCHIFANO, SEBASTIANO FABIO & TOSCHI, FEDERICO 2022 Build up of yield stress fluids via chaotic emulsification. *Journal of Turbulence* pp. 1–11.
- GOPALAN, BALAJI & KATZ, JOSEPH 2010 Turbulent shearing of crude oil mixed with dispersants generates long microthreads and microdroplets. *Physical review letters* **104** (5), 054501.
- HINZE, J. O. 1955 Fundamentals of the hydrodynamic mechanism of splitting in dispersion processes. *AIChE Journal* **1** (3), 289–295.
- II, SATOSHI, SUGIYAMA, KAZUYASU, TAKEUCHI, SHINTARO, TAKAGI, SHU, MATSUMOTO, YOICHIRO & XIAO, FENG 2012 An interface capturing method with a continuous function: The THINC method with multi-dimensional reconstruction. *Journal of Computational Physics* **231** (5), 2328–2358.
- KILPATRICK, PETER K 2012 Water-in-crude oil emulsion stabilization: review and unanswered questions. *Energy & Fuels* **26** (7), 4017–4026.
- KOKAL, SUNIL LALCHAND & OTHERS 2005 Crude oil emulsions: A state-of-the-art review. *SPE Production & facilities* **20** (01), 5–13.
- KOLMOGOROV, ANDREY 1949 On the breakage of drops in a turbulent flow. *Dokl. Akad. Navk. SSSR* **66**, 825—828.
- LI, MING & GARRETT, CHRIS 1998 The relationship between oil droplet size and upper ocean turbulence. *Marine Pollution Bulletin* **36** (12), 961–970.
- MANDAL, AJAY, SAMANTA, ABHIJIT, BERA, ACHINTA & OJHA, KEKA 2010 Characterization of oil-water emulsion and its use in enhanced oil recovery. *Industrial & Engineering Chemistry Research* **49** (24), 12756–12761.
- McCLEMENTS, DAVID JULIAN 2015 Food emulsions: principles, practices, and techniques. CRC press.
- MININNI, P. D., ALEXAKIS, A. & POUQUET, A. 2006 Large-scale flow effects, energy transfer, and self-similarity on turbulence. *Physical Review E - Statistical, Nonlinear, and Soft Matter Physics* **74** (1), 1–13.
- MUKHERJEE, SIDDHARTHA, SAJDARI, ARMAN, SHARDT, OREST, KENJERES, SASA, DEN AKKER, HARRY E. A. VAN, KENJEREŞ, SAŞA & VAN DEN AKKER, HARRY E.A. 2019 Droplet-turbulence interactions and quasi-equilibrium dynamics in turbulent emulsions. *Journal of Fluid Mechanics* **878**, 221–276, arXiv: 1902.09929.
- NIELLOUD, FRANÇOISE 2000 Pharmaceutical emulsions and suspensions: revised and expanded. CRC Press.

- OLIVIERI, STEFANO, CANNON, IANTO & ROSTI, MARCO E. 2022 The effect of particle anisotropy on the modulation of turbulent flows. *Journal of Fluid Mechanics* **950**.
- PANDEY, VIKASH, MITRA, DHRUBADITYA & PERLEKAR, PRASAD 2022 Turbulence modulation in buoyancy-driven bubbly flows. *Journal of Fluid Mechanics* **932**, 1–21.
- PANDEY, VIKASH, RAMADUGU, RASHMI & PERLEKAR, PRASAD 2020 Liquid velocity fluctuations and energy spectra in three-dimensional buoyancy-driven bubbly flows. *J. Fluid Mech* **884**, 6.
- PERLEKAR, PRASAD 2019 Kinetic energy spectra and flux in turbulent phase-separating symmetric binary-fluid mixtures. *Journal of Fluid Mechanics* **873**, 459–474.
- PERLEKAR, PRASAD, BENZI, ROBERTO, CLERCX, HERMAN J.H., NELSON, DAVID R. & TOSCHI, FEDERICO 2014 Spinodal decomposition in homogeneous and isotropic turbulence. *Physical Review Letters* **112** (1), 1–5.
- QI, YINGHE, TAN, SHIYONG, CORBITT, NOAH, URBANIK, CARL, SALIBINDLA, ASHWANTH KR & NI, RUI 2022 Fragmentation in turbulence by small eddies. *Nature Communications* **13** (1), 1–8.
- RIVIÈRE, ALIÉNOR, MOSTERT, WOUTER, PERRARD, STÉPHANE & DEIKE, LUC 2021 Sub-Hinze scale bubble production in turbulent bubble break-up. *Journal of Fluid Mechanics* **917**, A40.
- ROSTI, MARCO E, GE, ZHOUYANG, JAIN, SUHAS S, DODD, MICHAEL S & BRANDT, LUCA 2020 Droplets in homogeneous shear turbulence. *J. Fluid Mech* **876**, 962–984.
- SOLIGO, GIOVANNI, ROCCON, ALESSIO & SOLDATI, ALFREDO 2019 Breakage, coalescence and size distribution of surfactant-laden droplets in turbulent flow. *Journal of Fluid Mechanics* **881**, 244–282.
- SPERNATH, AVIRAM & ASERIN, ABRAHAM 2006 Microemulsions as carriers for drugs and nutraceuticals. *Advances in colloid and interface science* **128**, 47–64.
- TRYGGVASON, GRÉTAR, SCARDOVELLI, RUBEN & ZALESKI, STÉPHANE 2011 Direct numerical simulations of gas–liquid multiphase flows. Cambridge University Press.
- VELA-MARTÍN, ALBERTO & AVILA, MARC 2021 Deformation of drops by outer eddies in turbulence. *Journal of Fluid Mechanics* **929**.
- WANG, CHENG, YI, LEI, JIANG, LINFENG & SUN, CHAO 2022 Turbulence drag modulation by dispersed droplets in taylor-couette flow: the effects of the dispersed phase viscosity. *arXiv preprint arXiv:2210.04500* .
- YI, LEI, TOSCHI, FEDERICO & SUN, CHAO 2021 Global and local statistics in turbulent emulsions. *Journal of Fluid Mechanics* **912**, A13, arXiv: 2011.00963.
- YOUSEFI, ALI 2022 Transport and mixing by finite-size particles in turbulent flows. PhD thesis, KTH Royal Institute of Technology.

Acknowledgements. MCE, GB and SM acknowledge the support from the Departments of Excellence grant (MIUR) and INFN22-FieldTurb. The authors acknowledge computer time provided by the National Infrastructure for High Performance Computing and Data Storage in Norway (Sigma2, project no. NN9561K) and by SNIC (Swedish National Infrastructure for Computing).

Funding. LB acknowledge the support from the Swedish Research Council via the multidisciplinary research environment INTERFACE, Hybrid multiscalemodelling of transport phenomena for energy efficient processes, Grant no. 2016-06119.

Declaration of interests. The authors report no conflict of interest.

Data availability statement. Data are available from the corresponding author upon reasonable request.